

Modification of the oxygen storage capacity of CeO₂–ZrO₂ mixed oxides after redox cycling aging

F. Fally^a, V. Perrichon^{a,*}, H. Vidal^b, J. Kaspar^b, G. Blanco^c, J.M. Pintado^c,
S. Bernal^c, G. Colon^d, M. Daturi^e, J.C. Lavalley^e

^a *Laboratoire d'Application de la Chimie à l'Environnement (LACE), UMR 5634, Université Claude Bernard Lyon 1, 43 Bd du 11 Novembre 1918, 69622 Villeurbanne Cedex, France*

^b *Dipartimento di Scienze Chimiche, Università di Trieste, Via Giorgieri 1, 34127 Trieste, Italy*

^c *Departamento de Química Inorgánica, Facultad de Ciencias, Universidad de Cádiz, Polígono Rio San Pedro, 11510 Puerto Real, Cádiz, Spain*

^d *Centre SPIN, ENS Mines, 158 Cours Fauriel, 42023 St. Etienne Cedex-2, France*

^e *Laboratoire de Catalyse et Spectrochimie, UMR 6506, ISMRA, 6 Bd du Maréchal Juin, 14050 Caen Cedex, France*

Abstract

High surface area CeO₂–ZrO₂ mixed oxides were treated at 900–950°C either under wet air or under successive reducing and oxidizing atmospheres in order to study the evolution of the oxygen storage capacity (OSC) of these solids after different aging treatments. Several complementary methods were used to characterize the redox behavior: temperature programmed reduction (TPR) by H₂, TPO, magnetic susceptibility measurements to obtain the Ce³⁺ content, FT-IR spectroscopy of adsorbed methanol and a method to compare the oxygen buffering capacity (OBC) of the oxides.

All the results confirm that the mixed oxides exhibit better redox properties than pure ceria, particularly after aging. The enhancement in the OSC at moderate temperature has to be related to a deeper penetration of the reduction process from the surface into the under-layers. Redox cycling aging promotes the reduction at low temperature of all the mixed oxides, the improvement being much more important for low surface area aged samples. The magnitude of this effect does not depend on the BET surface areas which have similar values after cycling. This underlines the critical influence that the preparation and activation procedure have on the final OSC behaviors of the ceria–zirconia mixed oxides. © 2000 Elsevier Science B.V. All rights reserved.

Keywords: CeO₂–ZrO₂ mixed oxides; Oxygen storage capacity; Redox aging

1. Introduction

The improved oxygen storage capacity (OSC) of CeO₂–ZrO₂ mixed oxides compared to CeO₂ is now a well established fact [1–6] and justifies their general use for three-way catalysis applications. OSC is rec-

ognized to improve the catalytic activity, and generally speaking, it is related to the capacity of a system to release or to retake oxygen, during the different rich or lean phases that occur during the regulation of the exhaust gases composition. For ceria supports, several factors contribute to decrease the OSC during aging, and sintering may be one of the important causes for the OSC loss [7]. However, for ceria–zirconia mixed oxides, it was observed that an aging or a reduction treatment at high temperature is beneficial for OSC

* Corresponding author. Tel.: +334-72-43-15-87;

fax: +334-72-44-81-14.

E-mail address: vincent.perrichon@univ-lyon1.fr (V. Perrichon)

[8–10]. Therefore, the objective of this study is to know further how the OSC is modified when these systems are submitted to classical aging under air or to successive redox cycles at high temperature.

The term OSC itself, or more generally the redox properties, may cover different characteristics of the oxides and there is no means to measure OSC in an absolute way since it depends on the technique and the conditions of measurements. However, the redox state of an oxide can be characterized by several distinct parameters such as the oxygen released, the oxygen vacancies or the number of Ce^{3+} ions. The oxygen species involved in the processes may also concern the surface or/and the bulk, be desorbed at high temperatures or require a reductant. Also, the kinetics of reduction or oxidation may vary with the aging treatments. Therefore, to investigate in detail the different aspects of OSC of a series of ceria–zirconia mixed oxides, it is necessary to use complementary techniques in order to characterize them with certainty. In this study, several experimental methods were used to characterize the redox behavior of these mixed oxides: TPR with a classical TCD detector or coupled with a mass spectrometer, TPO, magnetic susceptibility measurements to obtain the Ce^{3+} content during redox treatments, FT-IR spectroscopy with a methanol probe allowing characterization of the surface and a method to compare the oxygen buffering capacity (OBC) of the oxides, i.e. the amount of oxygen of the oxide that can be exchanged with the surrounding atmosphere. We present the results obtained after high temperature aging (900–950°C) either under oxidizing or reducing atmosphere in order to reproduce the exhaust gas oscillations between fuel lean and fuel rich compositions. In order to have cubic or related to the ceria cubic phase starting materials [11], the study was limited to mixed oxides with a Ce content ≥ 50 at.%.

2. Experimental

The starting CeO_2 – ZrO_2 oxide samples were supplied by Rhodia. In addition to pure ceria, three mixed oxides were studied corresponding to the following nominal compositions expressed as Ce/Zr molar ratio, CZ-80/20, CZ-68/32 and CZ-50/50. The initial solids were homogeneous and their specific surface areas were close to $100 \text{ m}^2 \text{ g}^{-1}$ (HS samples). Details on

Table 1
General properties of the ceria–zirconia mixed oxides

Sample	Molar composition		Number of redox cycles	S_{BET} ($\text{m}^2 \text{ g}^{-1}$)
	Ce (at.%)	Zr (at.%)		
CZ-100/0-HS	100	0	0	100
CZ-100/0-LS			0	20
CZ-80/20-HS	80.2	19.8	0	111
			1	25
			3	16
CZ-80/20-LS			0	15
			1	15
			3	13
CZ-68/32-HS	68.2	31.8	0	100
			1	63
			3	28
CZ-68/32-LS			0	23
			1	21
			3	20
CZ-50/50-HS	50	50	0	106
			1	41
			3	22
CZ-50/50-LS			0	21
			1	18
			3	17

their textural and structural characterization are given elsewhere [11]. Their exact compositions are given in Table 1 with their BET surface areas.

In order to minimize the differences between the samples studied by each laboratory, standard aging treatments were applied to the oxide samples.

1. The LS samples were prepared by aging the initial HS oxides for 140 h at 900°C under wet air and then cooling to ambient temperature (rt). The BET surface area was lowered to about $20 \pm 5 \text{ m}^2 \text{ g}^{-1}$ (Table 1). Note that the surface area obtained with ceria is rather high ($20 \text{ m}^2 \text{ g}^{-1}$) and comparable to those of ceria–zirconia. From the literature, it is known that ceria exhibits a rather low thermal stability. For example, in a previous study on another ceria sample from Rhône–Poulenc, it was observed that the surface area dropped from 115 to $5 \text{ m}^2 \text{ g}^{-1}$ after a less severe treatment (6 h at 850°C under air) [12]. The higher stability obtained in the present study after a

thermal treatment at 900°C must be attributed to an improved preparation process as described in [13].

2. A second aging procedure based on redox cycling was applied to the HS and LS series. It consisted of 1 h reduction at 950°C under a flow of H₂(5%)/Ar, followed by a treatment under Ar at the same temperature and cooling to rt. Afterwards, the oxidizing part of the cycle was carried out by heating for 1 h at 550°C under flowing O₂(5%)/He and then low cooling under the same atmosphere to 150°C and desorption at this temperature. This cycling treatment was carried out either once or three times (referred as 1C or 3C). As shown in Table 1, the surface areas of the HS samples decreased significantly after the successive redox cycles, whereas almost no change was observed for the LS series.

Before each experiment and for each technique, the sample was also systematically pretreated according to the standard conditions defined previously [14]. In fact, they correspond to those adopted for the oxidizing part of the redox cycle, i.e. heating in a flow of O₂(5%)/He at 10°C min⁻¹ up to 550°C (1 h) and then cooling to 150°C for evacuation. In this way, a reproducible oxidation state could be obtained for the oxides with an almost clean surface. In the case of the magnetic balance, the samples were evacuated directly at 550°C after the oxidation treatment, since no significant change in the Ce³⁺ content was observed after evacuation at 150 or 550°C.

The TPR experiments were carried out by passing H₂(5%)/Ar at a flow rate of 25 ml min⁻¹ (heating rate 10°C min⁻¹) from rt to 1000°C over the standardized oxide (50 mg). A TCD device monitored the H₂ consumption. Experiments with a mass spectrometer were performed to confirm the results by analyzing the water formation. Oxygen uptake measurements were also performed in the same system by injecting oxygen pulses (0.125 ml) every 75 s on the catalyst, either at rt or at 427°C.

Magnetic susceptibility were obtained using a Faraday microbalance in order to follow the reduction of the diamagnetic Ce⁴⁺ ions of the mixed oxides into paramagnetic Ce³⁺ species. After the standard pretreatment, the reduction was performed step by step for 1 h at different increasing temperatures under H₂(5%)/He flow. The maximum temperature studied was 700°C. Each measurement was done after cooling the sample at rt under the same atmosphere and

the magnetic susceptibility was calculated according to the usual procedure and after extrapolation at infinite field [15]. The percentage of Ce³⁺ was calculated using the Curie–Weiss law determined on Ce₂O₃ [16].

The OBC technique consisted of injecting 0.25 ml pulses of O₂(5%)/He at high frequency (0.1 Hz) into a flow of He (60 ml min⁻¹) passing through the sample (200 mg). The oscillations in the oxygen pressure were followed by a TCD device. The attenuation of the signal was a measure of the OBC, ranging from 0 to 100% [17]. The measurement was done between rt and 900°C.

For the IR studies of adsorbed methanol, the sample was pressed into a disk (ca. 10 mg cm⁻²). All the activation, reduction and adsorption treatments were performed in situ in a quartz cell. Spectra were recorded at rt with a Nicolet Magna 550 FT-IR spectrometer and treated using the Nicolet OMNICTM software.

3. Results

3.1. TPR study of the reducibility of the mixed oxide

Fig. 1 gives the TPR profiles obtained with TCD analysis on the CZ-LS samples, i.e. after aging the HS

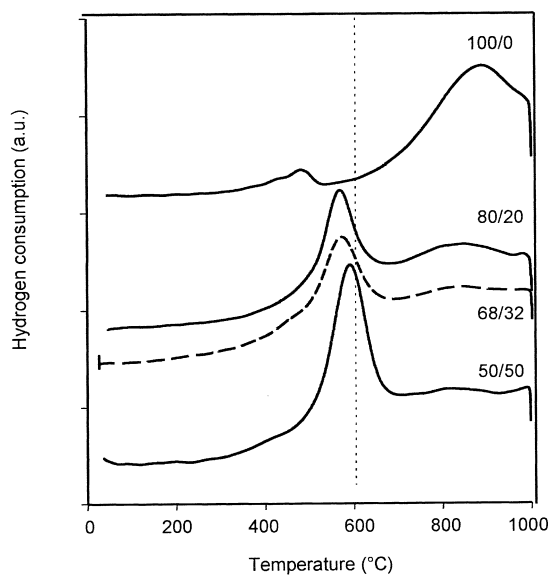


Fig. 1. Comparison of the TPR profiles of the ceria–zirconia LS samples.

samples under air. The curve for ceria presents two peaks at 480 and 895°C. In a simple approach, they can be attributed to the successive reduction of the surface and the bulk of ceria [18,19]. For the mixed oxides, only one peak is observed, with a maximum at 570–590°C, the temperature of which increases with the zirconium content. At higher temperatures, some H₂ consumption can be noticed, but with a lower extent than for ceria. The TPR profiles also show that for the CZ samples the H₂ consumption starts at lower temperatures than for ceria and that if the main peak can be tentatively adjusted in two peaks, there is no evident distinction between the surface and the bulk as it is for ceria. Since the surface areas of the LS oxides are not very different, it is clear that compared to ceria, the main peak corresponds to a much higher H₂ uptake than that needed for the surface reduction. It implies that several layers of the mixed oxide contribute to this peak and that the mobility of the involved oxygen atoms, although originated from the bulk is close to that of the ceria surface. It must be mentioned that these features are identical to those observed for the initial CZ-HS samples, except the intensity of the main H₂ peak which is lower for the aged oxides [20].

The influence of redox cycles was studied *in situ* by performing the reoxidation at 427°C at the end of each TPR, after 30 min at 1000°C (15 min under H₂(5%)/Ar and 15 min under pure Ar). Figs. 2 and 3 are related to the consecutive TPR carried out on CZ-100/0 and on CZ-68/32 chosen as typical examples. Both HS and LS samples were examined in order to study the influence of the surface area. For ceria, the profile for the HS sample is almost the same as already observed for a similar oxide [21]. It is clear that decreasing the surface area from HS to LS lowers the hydrogen uptake of the low temperature peak. The small differences in the profiles and the nonsymmetrical shape of this peak can be attributed to the presence of impurities as carbonates held by the ceria surface [19,21]. For both HS and LS samples reduced at 1000°C, the TPR 2 and TPR 3 profiles give evidence of the almost complete elimination of the low temperature surface reduction peak, whereas the peak related to the ceria bulk reduction remains almost unchanged throughout the cycles. The absence of a surface reduction peak accounts for a strong sintering of ceria reduced at 1000°C in agreement with the low thermal stability previously observed for CeO₂ under reducing conditions [12].

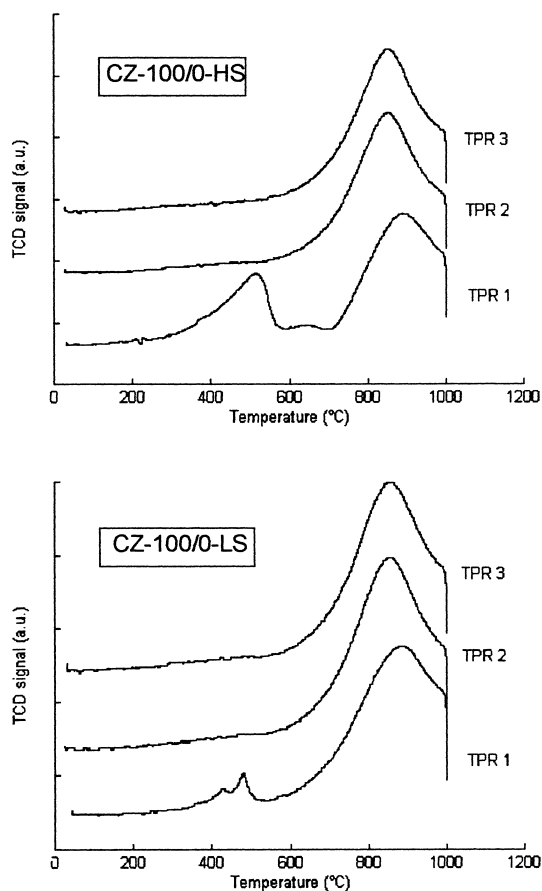


Fig. 2. Consecutive TPR performed on CZ-100/0-HS and CZ-100/0-LS cerium oxide. After each TPR up to 1000°C, the samples were reoxidized at 427°C.

For the CZ-68/32-HS and LS samples, there is essentially one peak at 570°C followed by a weak hydrogen uptake at high temperature, stronger on the CZ-68/32-LS sample compared to CZ-68/32-HS. It indicates that to fulfill the reduction, higher reduction temperatures are required for the low surface area sample. This lower reducibility is probably ascribable to the change in the texture of the solid. The slight structural modifications of the sample observed after the treatment at 900°C under air may also be considered [11]. During the successive TPR, the peak at 570°C practically remains unchanged in its position and its intensity, but develops a shoulder on the low temperature side, evidencing an improvement of the reducibility after redox cycling. It must be underlined

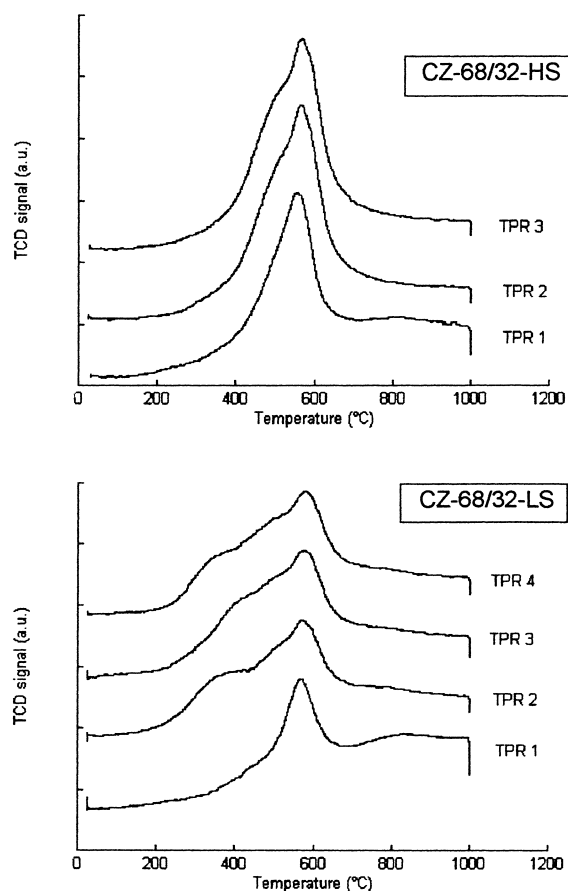


Fig. 3. Consecutive TPR performed on CZ-68/32-HS and CZ-68/32-LS ceria-zirconia mixed oxide. After each TPR up to 1000°C, the samples were reoxidized at 427°C.

that, at the same time, the BET surface area of the CZ-68/32-HS sample decreases from 100 to 63 and 28 m² g⁻¹ after one and three redox cycles, respectively. Thus, improved redox properties are obtained in spite of a much lower surface area, indicating the absence of a direct relationship between the BET surface area and the redox properties. The same observations can be seen for the CZ-68/32-LS sample. In this case, the BET surface area does not change (from 23 to 21 m² g⁻¹) but the low temperature reducibility of the oxide is improved by redox cycling, as evidenced by a pronounced shoulder appearing at 350–400°C on the TPR profile. Moreover, the comparison between the profiles for the HS and the LS samples indicates that the improvement at low temperature is much

better for the LS mixed oxide. Thus, although the initial oxidizing treatment at 900°C of the HS samples decreases its reducibility, it seems to be favorable for the subsequent reducibility improvement obtained after redox cycling.

3.2. Quantitative and kinetic aspects of the OSC

To avoid artifacts due to H₂ adsorption/desorption, we have directly measured the OSC by oxidizing the sample at 427°C after each TPR run [2]. Preliminary experiments were carried out by introducing oxygen pulses at rt until no more O₂ uptake was detected and then by performing a TPO up to 1000°C. It was observed that most of the oxidation took place at rt, with some complementary oxidation at around 100°C. Complete reoxidation was obtained at 427°C for all the samples, i.e. no additional O₂ was adsorbed by the oxide at higher temperatures. Thus, the O₂ uptakes at 427°C can be considered as a measure of the OSC-1000°C, i.e. the amount of oxygen vacancies created by the reduction at 1000°C. The results are given in Table 2 for all oxides studied. Three main conclusions can be established:

- The OSC after reduction at 1000°C is not modified by aging under air or redox cycling at high temperature although the BET surface area has largely decreased. This absence of variation has to be related to the high temperature reduction, since it has been shown in Figs. 2 and 3 that the TPR profiles exhibit no marked difference for $T > 800^\circ\text{C}$. Thus, at 1000°C, the maximum of transferable oxygen has been achieved and it does not vary with aging. The only exception is the case of CZ-50/50-LS sample, for which aging has decreased significantly the OSC value. It could be related to structural changes since the transition from a cubic to a tetragonal structure is observed at this composition [11].
- OSC is higher for the mixed oxides than for ceria. Moreover, expressed per gram of oxide or on a molar basis ($\text{Ce}_m\text{Zr}_{1-m}\text{O}_x$), it does not vary too much for zirconium content comprised between 20 and 50%.
- If OSC is expressed in the Ce³⁺ ion content, the reduction percentage at 1000°C increases with the zirconium content, evidencing the influence of the chemical composition on the reducibility of the cerium ions.

Table 2
O₂ uptake measured at 427°C for the CZ-HS and CZ-LS samples subjected to TPR up to 1000°C

Sample	Number of redox cycles	O ₂ uptake ^a (mmol g ⁻¹)	x in Ce _m Zr _{1-m} O _x ^b	Ce ³⁺ (%) ^b
CZ-100/0-HS	0	0.55	1.81	37.9
	1	0.57	1.80	39.5
	2	0.57	1.80	39.2
CZ-100/0-LS	0	0.58	1.80	40.2
	1	0.58	1.80	40.1
	2	0.55	1.81	37.6
CZ-80/20-HS	0	0.67	1.78	54.2
	1	0.70	1.77	56.7
	2	0.69	1.78	55.9
CZ-80/20-LS	0	0.69	1.78	55.9
	1	0.68	1.78	55.5
	2	0.70	1.77	56.5
CZ-68/32-HS	0	0.72	1.78	65.8
	1	0.73	1.77	67.5
	2	0.72	1.77	66.7
CZ-68/32-LS	0	0.72	1.77	66.2
	1	0.71	1.78	65.3
	2	0.72	1.77	66.2
	3	0.73	1.77	67.2
CZ-50/50-HS	0	0.74	1.78	87.1
	1	0.73	1.78	86.5
	2	0.73	1.78	86.5
CZ-50/50-LS	0	0.62	1.82	73.1
	1	0.65	1.81	76.6
	2	0.66	1.81	78.0

^a Standard deviation: ±0.01 mmol g⁻¹.

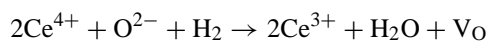
^b Estimated from the O₂ uptake.

Differences between the samples were also observed in the kinetics of reoxidation at 427°C. Fig. 4 gives the cumulative O₂ uptakes expressed in mmol O₂ per mmol oxide vs the number of pulses in the case of the LS series. The reoxidation process is slightly slower for the 80/20 and 68/32 compositions than for pure ceria or the CZ-50/50. Compared to the initial HS samples, it was found that the LS samples have slower reoxidation kinetics. Moreover, the O₂ uptake rate slightly decreases after the second and the third TPR at 1000°C. This trend is opposite to that observed for the reducibility behavior, since redox cycling promotes the reduction.

3.3. Magnetic balance study

The OSC was measured by determining the Ce³⁺ ion content of the mixed oxides after 1 h reduction at

different temperatures between rt and 700°C in flowing H₂(5%)/He using magnetic balance. The formation of oxygen vacancies V_O can be associated with the reduction of Ce⁴⁺ ions into Ce³⁺ ions according to the following reaction:



Thus, by determining the magnetic susceptibility and then the Ce³⁺ content, one can estimate the corresponding OSC. Moreover, with 1 h reduction time at each step, one can consider that a quasi-equilibrium OSC at each temperature is obtained. It must be mentioned that for better precision, the measurements were performed at rt under H₂/He. The reversible H₂ adsorption process which may account for only a few percent in the Ce³⁺ content [22] was not taken into account in the present study and its contribution neglected in the OSC values reported hereafter.

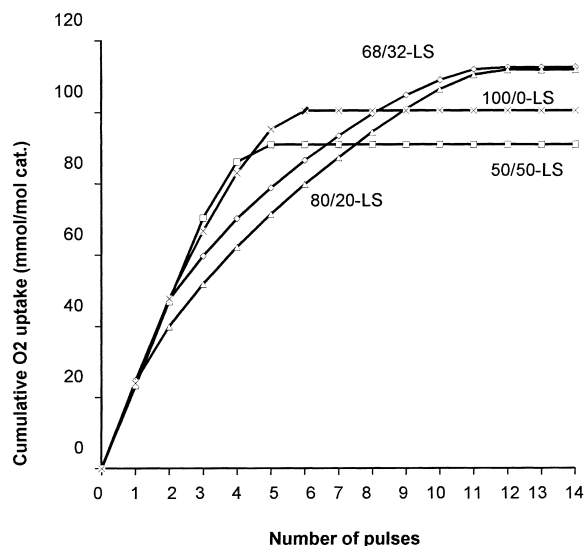


Fig. 4. Cumulative evolution of the O₂ uptake during the pulse experiments carried out over the CZ-LS oxides at 427°C.

The results concerning the LS samples are given in Fig. 5 and compared with those determined in the same conditions on the HS series [20]. In agreement with the TPR results, the reducibility of the oxides increases with the zirconium content. Moreover, at moderate temperatures, the reducibility of the LS mixed oxides is clearly lower than that of the HS samples. Thus, aging the HS mixed oxides under air at 900°C

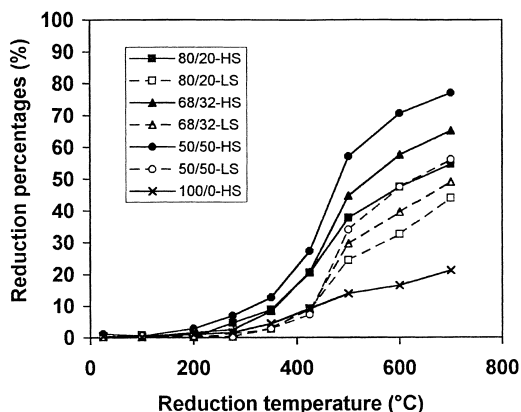


Fig. 5. Cerium reduction percentages ($100\text{Ce}^{3+}/\text{Ce}^{3+}+\text{Ce}^{4+}$) of the CZ-LS and HS mixed oxides determined from the magnetic susceptibility as a function of the reduction temperature (1 h at each temperature).

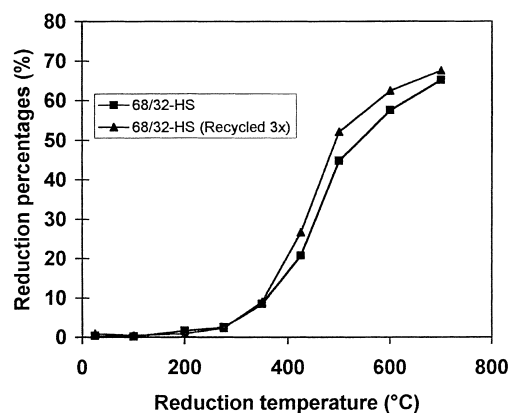


Fig. 6. Cerium reduction percentages ($100\text{Ce}^{3+}/\text{Ce}^{3+}+\text{Ce}^{4+}$) vs reduction temperature of the CZ-68/32-HS mixed oxide: influence of three redox cycling.

decreases the surface area by a factor around 5, and at the same time diminishes the redox properties.

The influence of redox cycling was studied on the 68/32 and 50/50 compositions. Although submission of CZ-68/32-HS to three redox cycles induces a decrease of surface area from 100 to $28\text{ m}^2\text{ g}^{-1}$, no change in the reduction percentage is observed after cycling for reduction temperature lower than 350°C (Fig. 6). At higher temperatures, the reducibility is slightly higher for the recycled sample, in agreement with the appearance of a shoulder on the TPR profile. For the oxide CZ-50/50-HS-3C (Fig. 7), the begin-

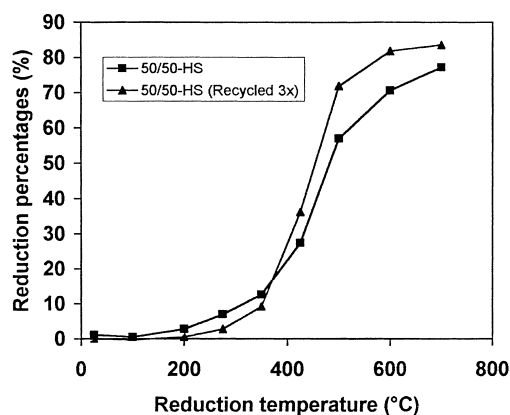


Fig. 7. Cerium reduction percentages ($100\text{Ce}^{3+}/\text{Ce}^{3+}+\text{Ce}^{4+}$) vs reduction temperature of the CZ-50/50-HS mixed oxide: influence of three redox cycling.

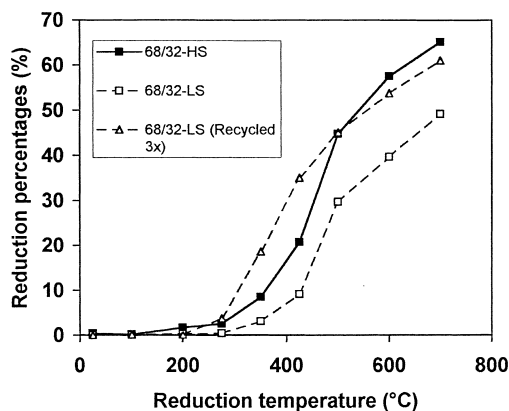


Fig. 8. Cerium reduction percentages ($100\text{Ce}^{3+}/\text{Ce}^{3+}+\text{Ce}^{4+}$) vs reduction temperature of the CZ-68/32-LS mixed oxide: influence of three redox cycling and comparison with the CZ-68/32-HS sample.

ning of reduction starts at a higher temperature, but an improvement of reducibility is observed for high reduction temperatures. Thus for the HS samples, redox cycling slightly improves the reducibility in spite of a lower BET surface area.

This enhancement is much more important for the LS series. Between 200 and 500°C, the reduction percentages, and therefore the OSC values, are even much higher than those observed for the corresponding HS samples (Figs. 8 and 9). The improvement of reducibility is observed after only one redox cycle, as evi-

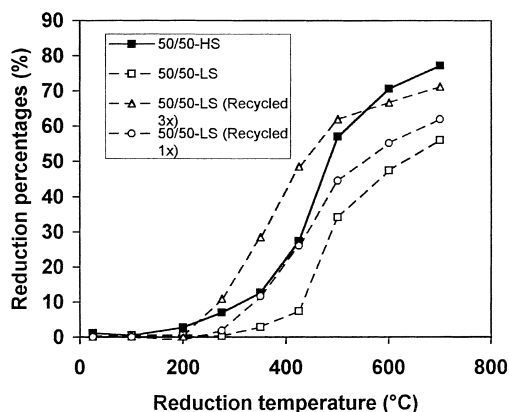


Fig. 9. Cerium reduction percentages ($100\text{Ce}^{3+}/\text{Ce}^{3+}+\text{Ce}^{4+}$) vs reduction temperature of the CZ-50/50-LS mixed oxide: influence of the number of redox cycling and comparison with the CZ-50/50-HS sample.

denced for CZ-50/50-LS-1C (Fig. 9). It is clear that the reducibility of the recycled mixed oxides is not controlled by the BET surface area.

TPO has shown that the oxidation of the reduced solids was occurring readily at rt. We have checked this point by introducing oxygen (6 kPa) at rt in the magnetic balance on the sample after reduction at 700°C and desorption under vacuum at 700°C. Table 3 gives the residual Ce^{3+} percentages after reoxidation of the samples at 25°C and after heating at 550°C, always under 6 kPa O_2 . All the reduced samples were easily oxidized by oxygen and the oxidation was nearly complete at 25°C for the HS samples while an additional heating treatment under oxygen was necessary to achieve full Ce^{3+} oxidation of the LS series and the recycled samples. In addition to the aging treatment, the chemical composition also influences the extent of reoxidation at rt. The latter increases when Zr content decreases. For CZ-50/50-LS, almost 10% of the cerium ions remain in the Ce^{3+} state after oxidation at rt. This relatively high content of cerium ions still remaining in the reduced state under O_2 at rt, again gives evidence of the slower reoxidation kinetics after redox cycling, contrary to the reducibility behavior. It is quite possible that the migration of the oxygen species is favored during the reduction step because reduction expands the structure due to the bigger size of the Ce^{3+} ion compared to the Ce^{4+} ion. On the contrary, when oxygen is introduced on the reduced sample, the oxidation of the first surface layers probably contracts the outer lattice, thus inhibiting the migration of oxygen in the bulk. It can also be supposed that since H_2 is a partner of the reduction, the diffusion of OH species could be favored compared to that of oxygen. However, as shown below, the same improvement of the redox properties after cycling is observed with the OBC measurements, although they are performed in the absence of hydrogen. Consequently, this second hypothesis does not seem determining.

Table 3 gives also the oxygen loss of the oxides after reduction at 700°C calculated from the Ce^{3+} percentages. These OSC values are a little lower than those obtained for the samples issued from TPR. It is consistent with the lower reduction temperature applied in the magnetic balance (700 instead of 1000°C). Calculated in mmol O_2 per gram of oxide, the highest OSC at 700°C was obtained for CZ-68/32-LS recycled 3 times (0.74 mmol g^{-1}).

Table 3

Ce³⁺ percentages obtained after reduction at 700°C under H₂(5%)/He, then after oxidation under oxygen (6 kPa) of the reduced samples, at 25°C and after oxidation at 550°C

Sample	Treatment conditions			
	After reduction at 700°C under H ₂ (5%)/He		At 25°C under O ₂ (6 kPa), Ce ³⁺ (%) ^a	After oxidation at 550°C under O ₂ (6 kPa), Ce ³⁺ (%) ^a
	Ce ³⁺ (%) ^a	O ₂ loss ^b (mmol g ⁻¹)		
CZ-100/0-HS	21.2	0.308		
CZ-80/20-HS	54.6	0.675	1.3	0.8
CZ-68/32-HS	65.1	0.709	1.5	0.7
CZ-50/50-HS	77.2	0.654	2.2	1.7
CZ-80/20-LS	44.0	0.544	1.9	1.1
CZ-68/32-LS	49.0	0.534	5.2	1.1
CZ-50/50-LS	56.0	0.474	9.9	2.6
CZ-68/32-HS-3C	67.5	0.735	6.1	1.5
CZ-50/50-HS-3C	83.6	0.708	5.0	1.7
CZ-68/32-LS-3C	61.1	0.665	3.3	1.4
CZ-50/50-LS-3C	71.3	0.604	2.6	0.8

^a Estimated from the magnetic susceptibility measurements.

^b Calculated from the Ce³⁺ percentages.

3.4. OBC measurements

The redox behavior of the CZ mixed oxides was also investigated by using the OBC technique in which pulses of O₂(5%)/He are injected every 10 s into a flow of helium passing through the mixed oxide [17]. Due to the interactions of the oxide with oxygen, the oscillations become attenuated and this attenuation measures the OBC. OBC is expected to increase with temperature, since more oxygen is supposed to become

available for redox processes at high temperature. Before running the OBC experiments, the samples were always submitted to the in situ standard pretreatment.

For ceria, no OBC can be measured below 950°C, for which the value is 5%. For the initial mixed oxides (HS series), the OBC is much higher and reaches values close to 80% at 900°C [20]. As shown in Fig. 10, aging the HS samples at 900°C under air to obtain the LS series lowers the OBC. The OBC also decreases when Zr content increases.

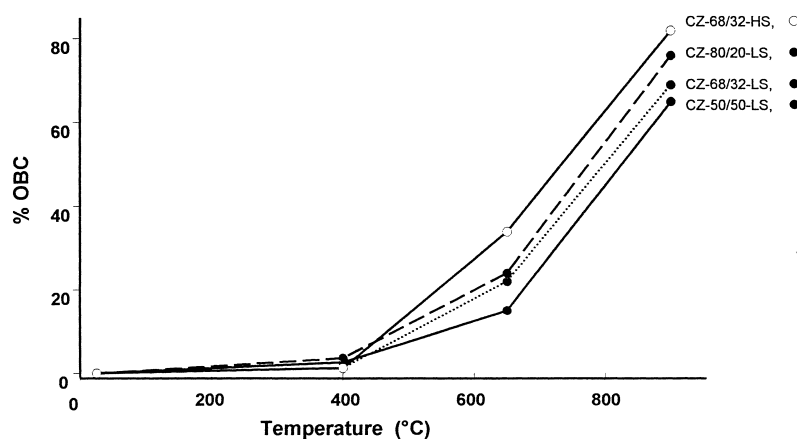


Fig. 10. OBC of the CZ samples measured at different temperatures: effect of aging under air and of the zirconium content.

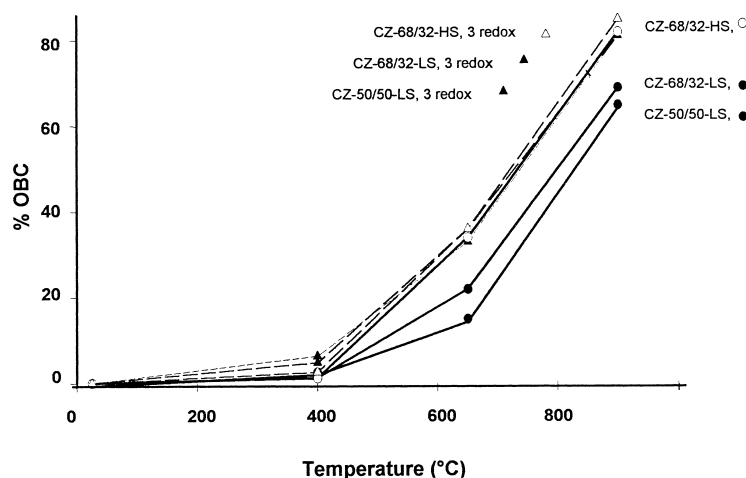


Fig. 11. OBC of the CZ samples measured at different temperatures: effect of redox cycling on HS and LS samples.

Redox cycling has a negligible effect on the OBC measured on the CZ-68/32-HS oxide in spite of a decrease of the surface area. At the same time, cycling increases the OBC of CZ-68/32-LS and CZ-50/50-LS (Fig. 11). Therefore, although no similar beneficial effect was found for the CZ-80/20-LS sample, the OBC of the aged LS oxides has been improved by redox cycling. It is in agreement with the TPR and magnetic balance results mentioned above and again gives evidence of the beneficial effect of the reducing treatment performed during the redox cycling.

3.5. Study of the surface by FT-IR measurements

Methanol is a very powerful molecular probe that can be used to study the surface of the CZ oxides by IR spectroscopy. Upon adsorption, it dissociates, giving selective coordination states on Zr and Ce cations, either in the oxidized or the reduced state. It has been found that OCH₃ groups are sensitive to the cationic site arrangement and to the reduction grade of the sample [23–25]. By following the evolution of the methoxy groups on the surface, it is possible to obtain information on the surface composition and on the different reduction steps of the oxide. In fact, as illustrated in Fig. 12A for the CZ-50/50-HS oxide, the band at 1155 cm⁻¹ is due to methoxy groups linearly coordinated over Zr⁴⁺ [26], while the band at 1105 cm⁻¹ represents methoxy groups linearly coordinated over

Ce⁴⁺ [23,24]. The peak around 1065 cm⁻¹ is assigned to bridged species [23,24]. The reciprocal intensity of the two bands of type I allows us to determine the cationic proportion at the surface [25].

After reduction of the sample by hydrogen treatment at 673 K, the surface presents the same features concerning exposed zirconium cations (Fig. 12B), zirconium not being reducible in these conditions. On the contrary methoxy groups are preferentially twofold coordinated over Ce³⁺ (peak II*, 1080 cm⁻¹), but they can also present a band around 1120 cm⁻¹ due to linear species over Ce³⁺. The reciprocal intensities of I (Ce) and II* bands allows us to estimate the surface reduction degree.

Thus, in order to give an evidence of a possible change in the surface chemistry when the oxide was submitted to redox cycling aging, we have studied the CZ-50/50-HS sample before and after three redox cycles. For the sake of clarity, spectra in Fig. 12 are not in the same scale, since the aged sample has a lower surface area, then a lower number of exposed adsorption sites. Nevertheless, it is interesting to notice that the integration of the bands due to methoxy species (both in the νOC or in the νCH stretching ranges) reveals that the thermal treatment has reduced the number of adsorbed molecules by a factor 2.5–3. On the contrary surface area has decreased by a factor 5. It seems, therefore that we have almost the double of the expected methoxy groups on the aged sample.

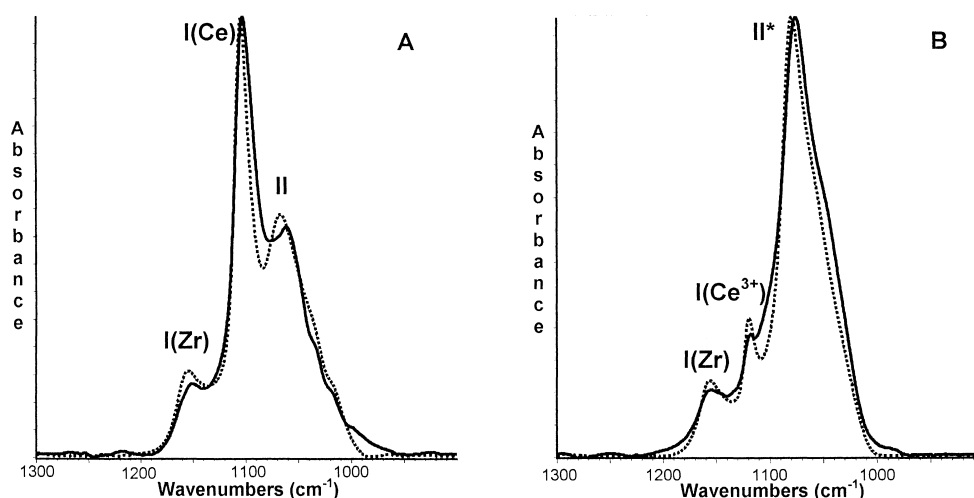


Fig. 12. FT-IR spectra of methoxy species on CZ-50/50-HS sample before (dotted lines) and after (full lines) three redox cycles. Methanol has been adsorbed at room temperature either on the (A) oxidized or (B) reduced surfaces.

The adsorption of methanol on the CZ-50/50-HS sample (Fig. 12A) after cycling (3C) reveals a virtually homogeneous distribution of Ce and Zr cations on the surface when compared with the fresh sample and suggests that there are no significant differences of surface chemical composition between the oxides. Nevertheless, a deeper analysis of the spectra indicates a slight lowering of the band assigned to linear species over zirconium, compensated by an increase of the type I (Ce) bandwidth in the cycled sample. This might suggest that cerium on the surface has slightly increased. A similar phenomenon can also be observed on the reduced sample (Fig. 12B). Furthermore, the overall, even if only slight, widening of the bands in the cycled sample and the small decrease of the I (Ce³⁺) feature could reveal a more heterogeneous surface.

Concerning the reduction process itself, the study of the shift in the ν_{OC} stretching wave number and of the overall intensity of this band has shown [27] that on the initial CZ-50/50-HS, the reduction by hydrogen begins at 250°C. A stable highly reduced state is reached at ca. 280°C and is maintained at least up to 600°C, independently from bulk reduction. The OSC measured on this mixed oxide after reduction at 300°C corresponds to that obtained at 500°C for pure ceria, suggesting a deeper penetration of the reduc-

tion process from the surface into the under-layers in agreement with the TPR and magnetic balance results.

When performed on the cycled aged sample, the OSC measurements have also shown that the reducibility after cycling has increased. However, a quantitative analysis was not possible. In fact, as described elsewhere [23,28], OSC evaluation by IR spectroscopy applied on methanol adsorption is based on the progressive reoxidation of the surface after introduction of successive well-known doses of O₂. In the case of the cycled sample, oxygen introduction leads to a sudden reoxidation of the surface, with local heat releasing and the consequent probe destruction. To avoid this problem, we have tried to use a weaker oxidizing agent, such as N₂O. In this case methanol resists on the surface, but we cannot obtain a complete reoxidation of the sample without heating it at least at 100°C under oxidizing atmosphere. In any case the OSC value measured before the reoxidation limit at room temperature is higher than for the untreated sample when reduced in the same conditions.

These results show that cycling could produce a surface with higher reactivity and, at the same time, a bulk-like more stable reduced state. Perhaps a structural distortion towards Ce₂O₃ phase or the formation of a superstructure should be hypothesized, as FT-IR

skeletal analysis seems to suggest. An investigation in this sense is in progress.

4. Discussion

The objective of this work was to put together an ensemble of techniques to study in detail the influence of aging on the redox properties of ceria–zirconia mixed oxides. The first point to underline is that the data obtained by TPR, OSC, OBC or magnetic balance are complementary and lead to convergent conclusions. In particular, the concordance of the results obtained by TPR–TPO and magnetic balance clearly shows that the measured Ce^{3+} ions content are associated with the formation of oxygen vacancies in the oxide. The IR and OBC results do not allow a direct comparison of the OSC values because they concern essentially the surface. However, the results obtained by adsorbing methanol on the reduced oxides show that the reduction of the surface is achieved at lower temperature on the mixed oxides than on ceria. This conclusion is in agreement with the bulk techniques which indicate a high mobility of the oxygen species not only at the surface but also in the bulk, this mobility increasing with the zirconium content.

This mobility also is modified by aging treatments. Aging under air at 900°C the HS mixed oxides with a high surface area decreases the BET surface area by a factor around 5. At the same time, the redox properties are somewhat lowered. Aging the same solids by a redox cycle, including first a reduction step at $900/1000^\circ\text{C}$ and then an oxidation at $427/550^\circ\text{C}$, leads to very different results. Whereas the BET surface area of the HS samples is progressively decreased by the successive cycles, the redox properties are preserved or even become slightly better as a consequence of redox aging. No quantitative data could be obtained on OSC with IR spectroscopy on the cycled sample because the reoxidation of the surface was too fast and destroyed the adsorbed methanol probe. However, IR spectra show that almost two times more sites adsorb methanol on the cycled sample. This suggests that there are more sites able to react on the surface of the cycled oxide which could explain the higher reactivity of this oxide in spite of a much lower surface. As discussed below, surface composition and surface structure are other important parameters.

For the LS series, i.e. HS samples aged under air, redox cycling improves the redox properties by increasing the reducibility at mild temperature ($T < 500^\circ\text{C}$), despite the surface area remaining constant. After three redox cycles, the improvement is very significant, and the OSC at mild temperature becomes the highest among the studied samples, including the HS series. Thus, the oxidizing aging treatment at 900°C of the HS samples would be a favorable parameter in the subsequent reducibility improvement obtained on redox cycling. This observation can be paralleled with the results obtained previously for CZ-68/32-LS which exhibits reversible changes in its redox properties by alternating the reoxidation temperature after reduction at 950°C [29]. Thus, after reduction at 950°C under pure H_2 , the sample reoxidized at mild temperature (550°C) exhibited better redox properties than if reoxidized at high temperature (950°C). This change in the redox properties was reversible and could be reproduced several times. In the present study, before each measurement, all the samples were standardized by an oxidizing treatment at $427\text{--}550^\circ\text{C}$, i.e. a mild oxidation treatment. After such a standardization, one should therefore obtain optimized redox properties for all the oxides. Consequently, the improvement observed after the redox cycles must certainly be attributed to the reduction step of the redox cycle.

If the pretreatment conditions appear to play a key role in determining the redox behavior of the resulting oxides, the chemical composition is also an important parameter. It is clear that the reducibility at low temperature is increased when the zirconium content increases. Thus, introduction of zirconium ions in the cubic ceria widens the operating window by favoring the reduction of the mixed oxide at low temperature. On a quantitative basis, OSC is not proportional to the Zr content, because the amount of oxygen available for the reduction is associated with the cerium ions and therefore this number decreases when Zr content increases. In fact, for the three compositions studied and for one specific type of treatment (aging or redox cycling), the OSC calculated in mmol O_2 per gram of oxide at a given temperature are very close. This suggests that any mixed oxide with a zirconium content between 20 and 50% would give a convenient support for TW catalysts. This remark is in agreement with previous observations which indicated that the OSC

at 400°C was the maximum for the intermediate ZrO₂ contents (25–50 mol%) [2].

In addition to the chemical composition, the surface chemistry is another parameter to discuss. As said previously, there is no direct relationship between OSC or OBC and the BET surface area. Moreover, the mixed oxide do not exhibit a reduction behavior characterized by well separated surface and bulk reduction steps as for ceria. These results indicate a high oxygen reactivity in the mixed oxides at low temperature, the difference between the surface and the bulk not being very great. The high mobility of the oxygen species is confirmed by the easiness of the oxidation of the reduced oxides that is almost complete at rt, as shown by the low Ce³⁺ content obtained after reoxidation. Notice, however, that an expanded lattice is present in the reduced CeO₂–ZrO₂ moiety [2]. This mobility has been shown to be increased by successive high temperature redox cycles, the effect being stronger for the LS than for the HS oxide. Since there is no significant change in the BET surface area, local modifications are probably involved to explain these differences. The results obtained with the methanol probe showed a surface cationic distribution not very different between the initial 50/50-HS sample and the cycled one. Only a slight enrichment of the surface in cerium ions was evidenced. Therefore, the interpretation is far from being evident. However, since the surface composition could be more heterogeneous, it can be supposed that the redox treatments induce nanostructural modifications which may improve the reducibility of the cerium ions in the first layers of the cycled oxides. XPS, structural and HREM studies are under progress in the CEZIRENCAT network and should help to verify this hypothesis.

5. Conclusion

Compared to pure ceria, the ceria–zirconia mixed oxides show improved reducibility, particularly at mild reducing conditions ($T < 500^\circ\text{C}$). It is clearly evidenced by the TPR profiles and the OSC values obtained for the HS and LS series and by the reduction curves obtained in the magnetic balance. The OSC values are a function of the temperature and time of the reduction. If the differences are leveled between the CZ samples when the OSC is

measured after reduction at 1000°C, more distinct behaviors are obtained at lower reduction temperature. FT-IR results, using OCH₃ species to probe the reduction extent of the sample, are also in agreement with this enhanced reducibility and easy reoxidation. Thus, for CZ-50/50-HS, the reduction started at 250°C and a highly reduced state of the surface could be observed at 300°C, compared to 500°C for ceria, suggesting a deeper penetration of the reduction process from the surface into the underlayers.

After aging of the HS samples under air at 900°C, the reducibility of the mixed oxides is depressed to some extent. More important is the effect of redox cycling which greatly improves the redox properties of both HS and LS ceria–zirconia mixed oxides, but particularly for the LS samples. The redox properties exhibited are independent of their BET surface areas which have similar values after cycling. The adsorption of methanol on the cycled sample also shows that there are almost two times more adsorbing sites than expected from the surface area values. These observations underline the critical influence that the preparation and activation procedure have on the surface chemistry and the final OSC behavior of the ceria–zirconia mixed oxides. It should be recalled that in this respect the reoxidation temperature has a decisive influence on the reducibility of these systems [29]. The origin of these modifications of reducibility is under study. IR results indicate that the surface composition could be slightly more heterogeneous after redox cycling. Therefore, the improvement of reducibility of the cerium ions in the first layers of the cycled oxides could be due to nanostructural changes in the oxide induced by the successive thermal treatments in reducing or oxidizing environments. A future publication from the CEZIRENCAT network, based in particular on structural and HREM studies, will discuss this hypothesis.

Acknowledgements

The authors are grateful to the European Commission for the financial support received from the TMR Program (CEZIRENCAT Project, Contract FMRX-CT-96-0060 (DG12-BIUO)).

References

- [1] T. Murota, T. Hasegawa, S. Aozasa, H. Matsui, M. Motoyama, *J. Alloys Compounds* 193 (1993) 298.
- [2] P. Fornasiero, R. Di Monte, G. Ranga Rao, J. Kaspar, S. Meriani, A. Trovarelli, M. Graziani, *J. Catal.* 151 (1995) 168.
- [3] J.P. Cuif, G. Blanchard, O. Touret, A. Seigneurin, M. Marczy, E. Quéméré, *SAE Paper* 970463 (1997).
- [4] C.E. Hori, H. Permana, K.Y.S. Ng, A. Brenner, K. More, K.M. Rahmoeller, D.N. Belton, *Appl. Catal. B* 16 (1998) 105.
- [5] J. Kaspar, P. Fornasiero, M. Graziani, *Catal. Today* 50 (1999) 285.
- [6] C. de Leitenburg, A. Trovarelli, F. Zamar, S. Maschio, G. Dolcetti, J. Llorca, *J. Chem. Soc., Chem. Commun.* (1995) 2181.
- [7] E. Rogemond, N. Essayem, R. Fréty, V. Perrichon, M. Primet, S. Salasc, M. Chevrier, C. Gauthier, F. Mathis, *Stud. Surf. Sci. Catal.* 116 (1998) 137.
- [8] H.W. Jen, G.W. Graham, W. Chun, R.W. McCabe, J.P. Cuif, S.E. Deutsch, O. Touret, *Catal. Today* 50 (1999) 309.
- [9] G. Balducci, P. Fornasiero, R. Di Monte, J. Kaspar, S. Meriani, M. Graziani, *Catal. Lett.* 33 (1995) 193.
- [10] P. Fornasiero, G. Balducci, R. Di Monte, J. Kaspar, V. Sergio, G. Gubitosa, A. Ferrero, M. Graziani, *J. Catal.* 164 (1996) 173.
- [11] G. Colon, M. Pijolat, F. Valdivieso, H. Vidal, J. Kaspar, E. Finocchio, M. Daturi, C. Binet, J.C. Lavalley, R.T. Baker, S. Bernal, *J. Chem. Soc., Faraday Trans.* 94 (1998) 3717.
- [12] V. Perrichon, A. Laachir, S. Abouarnadasse, O. Touret, G. Blanchard, *Appl. Catal. A* 129 (1995) 69.
- [13] J.L. Le Loarer, F. Picard, C. David, *Patent Application No. FR8817069* (1988).
- [14] M. Daturi, C. Binet, J.C. Lavalley, H. Vidal, J. Kaspar, M. Graziani, G. Blanchard, *J. Chem. Phys.* 95 (1998) 2048.
- [15] J.P. Candy, V. Perrichon, *J. Catal.* 89 (1984) 93.
- [16] T. Sata, M. Yoshimura, *J. Ceram. Assoc. Jpn.* 76 (1968) 30.
- [17] S. Bernal, G. Blanco, M.A. Cauqui, P. Corchado, J.M. Pintado, J.M. Rodriguez-Izquierdo, *J. Chem. Soc., Chem. Commun.* (1997) 1545.
- [18] H.C. Yao, Y.F. Yu Yao, *J. Catal.* 86 (1984) 254.
- [19] V. Perrichon, A. Laachir, G. Bergeret, R. Frety, L. Tournayan, O. Touret, *J. Chem. Soc., Faraday Trans.* 90 (1994) 773.
- [20] H. Vidal, J. Kaspar, M. Pijolat, G. Colon, S. Bernal, A. Cordon, V. Perrichon, F. Fally, *Appl. Catal. B*, accepted for publication.
- [21] F. Fajardie, J.F. Tempere, J.M. Manoli, G. Djega-Mariadassou, G. Blanchard, *J. Chem. Soc., Faraday Trans.* 94 (1998) 3727.
- [22] M. Daturi, E. Finocchio, C. Binet, J.C. Lavalley, F. Fally, V. Perrichon, *J. Phys. Chem. B* 103 (1999) 4884.
- [23] C. Binet, M. Daturi, J.C. Lavalley, *Catal. Today* 50 (1999) 207.
- [24] A. Badri, C. Binet, J.C. Lavalley, *J. Chem. Soc., Faraday Trans.* 93 (1997) 1159.
- [25] M. Daturi, C. Binet, J.C. Lavalley, A. Galtayries, R. Sporcken, *PCCP* 1 (1999) 5717.
- [26] F. Ouyang, N. Kondo, K.I. Maruya, K. Domen, *J. Phys. Chem. B* 101 (1997) 4867.
- [27] M. Daturi, E. Finocchio, C. Binet, J.C. Lavalley, F. Fally, V. Perrichon, H. Vidal, N. Hickey, J. Kaspar, *J. Phys. Chem. B*, submitted for publication.
- [28] E. Finocchio, M. Daturi, C. Binet, J.C. Lavalley, F. Fally, V. Perrichon, H. Vidal, J. Kaspar, M. Graziani, G. Blanchard, *Stud. Surf. Sci. Catal.* 121 (1999) 257.
- [29] R.T. Baker, S. Bernal, G. Blanco, A.M. Cordon, J.M. Pintado, J.M. Rodriguez-Izquierdo, F. Fally, V. Perrichon, *J. Chem. Soc., Chem. Commun.* (1999) 149.